Path and life predictions under mixed mode I-Mode II complex loading

A.C.O. Miranda, M.A. Meggiolaro, J.T.P. Castro
Mechanical Engineering Department, Pontifical Catholic University of Rio de Janeiro, RJ – Brazil

L.F. Martha
Civil Engineering Department, Pontifical Catholic University of Rio de Janeiro, RJ – Brazil

Abstract

A hybrid global-local methodology to predict fatigue crack path and propagation life in 2D structures is extended to model crack retardation effects induced by variable-amplitude (VA) loading histories. First, finite element (FE) models are used at each propagation step to calculate the generally curved fatigue crack path. However, the FE approach alone is not computationally efficient to predict crack growth rate, because it would require time-consuming remeshing of the entire structure after each event in VA loading. Therefore, the crack path and their mixed-mode stress intensity factors are FE calculated under constant-amplitude (CA) loading using fixed crack increments, requiring only relatively few remeshing steps. An analytical expression is then fitted to the calculated $\mathbf{K}_I$ values, which is used in a powerful general purpose local-approach fatigue design program to predict crack propagation lives under VA loading, considering load interaction effects such as crack retardation or arrest after overloads. This methodology is experimentally validated by fatigue crack growth tests on compact tension C(T) specimens, modified with holes positioned to attract or to deflect the fatigue cracks. Experiments under VA loading are also performed on C(T) specimens without holes. Several crack retardation models are calibrated based on straight-crack data. These models are then used to successfully predict the curved crack growth behavior under VA loading of the hole-modified specimens.

1 Introduction

Fatigue life prediction of cracked two-dimensional (2D) structural components requires the calculation of the generally curved crack path, the associated stress intensity factors (SIF) $\mathbf{K}_I$ and $\mathbf{K}_{II}$, and the crack propagation rate at each load step [1]. A finite element (FE) global discretization of the component, using specialized crack tip elements to predict the crack path and to calculate its associated SIF, is a standard practice. However, this global calculation method is not computationally efficient

Mechanics of Solids in Brazil 2007, Marcílio Alves & H.S. da Costa Mattos (Editors)
Brazilian Society of Mechanical Sciences and Engineering, ISBN 978-85-85769-30-7

under variable amplitude (VA) loading to predict fatigue lives, because it requires time-consuming remeshing procedures and FE recalculations after each loading event.

On the other hand, the so-called local approach, based on the direct integration of a crack propagation rule such as **da/dN = F(ΔK, R, ...)**, can be efficiently used to calculate the crack increment at each load cycle, considering crack retardation effects if necessary (**da/dN** is the crack growth rate, **ΔK** the SIF range and $\mathbf{R} = \mathbf{K}_{min}/\mathbf{K}_{max}$). However, this approach requires the SIF expression for the cracked geometry, which simply is not available for most real components.

Since the advantages of these two approaches are complementary, the problem can be divided into two steps. First, the curved fatigue crack path and its SIF are calculated under constant amplitude (CA) loading in a specialized FE program, using small crack increments and automatic remeshing. Numerical methods are used to calculate the crack propagation path, based on the computation of the crack incremental direction, and the associated SIF $\mathbf{K}_I(\mathbf{a})$ and $\mathbf{K}_{II}(\mathbf{a})$, where **a** is the length along the crack path. The $\mathbf{K}_I(\mathbf{a})$ values are then used as an input to a fatigue program based on the local approach, where the actual VA loading is efficiently treated by the integration of the crack propagation equation, considering overload-induced retardation effects if required [1].

In this work, fatigue crack growth experiments under VA loading are performed on compact tension C(T) specimens made of cold-rolled SAE 1020 steel, modified with holes positioned to attract or to deflect the fatigue cracks. The curved crack paths are FE-predicted under CA loading, resulting in good estimates of the measured paths under VA loading. The results suggest that overloads do not deviate significantly the crack path predicted under constant amplitude loading, provided that the overload does not induce crack bifurcation or plastic zones with sizes comparable to the residual ligament. Experiments under VA loading are also performed on C(T) specimens without holes. Several crack retardation models are calibrated based on straight-crack data. These models are then used to successfully predict the curved crack growth behavior under VA loading of the hole-modified specimens.

2 Mixed-mode crack growth calculations

In FE mixed-mode crack growth calculations, three methods are generally used to compute the stress intensity factors along the (generally curved) crack path: the displacement correlation technique [2], the potential energy release rate computed by means of a modified crack-closure integral technique [3, 4], and the J-integral computed by means of the equivalent domain integral (EDI) together with a mode decomposition scheme [5, 6]. The EDI method replaces the J-integral along a contour by another one over a finite size domain, using the divergence theorem, which is more convenient for FE analysis.

Since Bittencourt et al. [7] showed that for sufficiently refined FE meshes all three methods predict essentially the same results, only the EDI method is considered in the calculations presented here. However, the other two methods also provide good results even for relatively coarse meshes.

The calculated Modes I and II SIF $\mathbf{K}_I$ and $\mathbf{K}_{II}$ are then used to obtain an equivalent SIF $\mathbf{K}_{eq}$. The fatigue crack growth rate can then be computed from the equivalent stress intensity range $\Delta\mathbf{K}_{eq}$ by a simple McEvily-type model [8]:

$$\frac{da}{dN} = A \cdot (\Delta K_{eq} - \Delta K_{th})^m \tag{1}$$

where $\Delta\mathbf{K}_{th}$ is the threshold SIF and **A** and **m** are the conventional tensile crack growth rate parameters for the given material. An alternative Elber-type equation can be used based on the maximum equivalent stress intensity $\mathbf{K}_{eq}$ and on the crack opening value $\mathbf{K}_{op}$, namely

$$\frac{da}{dN} = A \cdot (K_{eq} - K_{op})^m \tag{2}$$

Several models have been proposed to obtain $\mathbf{K}_{eq}$ from $\mathbf{K}_I$ and $\mathbf{K}_{II}$ (and $\mathbf{K}_{III}$, when it is important). E.g., Tanaka [9] obtained an equivalent stress intensity model based on the displacements behind the crack tip reaching a critical value, leading to

$$K_{eq} = \left[K_I^4 + 8 \cdot K_{II}^4 + \frac{8 \cdot K_{III}^4}{1-\nu}\right]^{1/4} \tag{3}$$

where ν is Poisson's coefficient.

Another expression for $\mathbf{K}_{eq}$ can be derived for elastic loading under plane stress conditions, based on the relations between the potential energy release rate **G** and the SIF [10], leading to

$$K_{eq} = \sqrt{K_I^2 + K_{II}^2 + (1+\nu) \cdot K_{III}^2} \tag{4}$$

Hussain et al. [11] used complex variable mapping functions to obtain **G** at a direction θ with respect to the crack propagation plane under Mode I and II combined loading. They assumed that crack extension occurs in a direction $\theta = \theta_0$ that maximizes **G**, leading to the Maximum Fracturing Energy Release Rate ($\mathbf{G}_{max}$) criterion. Thus, an equivalent SIF is obtained at $\theta = \theta_0$ that maximizes

$$K_{eq} = \sqrt{\frac{4}{(3+\cos^2\theta)^2}\left(\frac{1-\theta/\pi}{1+\theta/\pi}\right)^{\theta/\pi}\left[(1+3\cos^2\theta)K_I^2 - 8\sin\theta\cos\theta \cdot K_I K_{II} + (9-5\cos^2\theta)K_{II}^2\right]} \tag{5}$$

The computed θ_0 values at each calculation step are used to obtain the crack incremental growth direction - and thus the fatigue crack path - in the linear-elastic regime.

Sih [12] proposed the Minimum Strain Energy Density $\mathbf{S}_{min}$ criterion, assuming that the crack propagates in a direction $\theta = \theta_0'$ that minimizes the strain energy **S** around the crack tip. The associated equivalent SIF is then calculated at $\theta = \theta_0'$ that minimizes the expression

$$\begin{aligned} K_{eq}^2 = \tfrac{1}{4(1-2\nu)}\{&(3-4\nu-\cos\theta)(1+\cos\theta)\cdot K_I^2 + 2\sin\theta\cdot[\cos\theta - 1 + 2\nu]\cdot K_I K_{II} + \\ &+[4(1-\nu)(1-\cos\theta) + (1+\cos\theta)(3\cos\theta-1)]\cdot K_{II}^2 + 4K_{III}^2\} \end{aligned} \tag{6}$$

Erdogan and Sih [13] proposed the Maximum Circumferential Stress ($\sigma_{\theta max}$) criterion, which considers that crack growth should occur in the direction that maximizes the circumferential stress in the

region close to the crack tip. They considered the stresses at the crack tip under combined Mode I and II loading, given by summing up the stress fields generated by each mode:

$$\sigma_r = \frac{1}{\sqrt{2\pi r}}\left\{\frac{1}{4}\left(5\cos\frac{\theta}{2} - \cos\frac{3\theta}{2}\right)\cdot K_I - \frac{1}{4}\left(5\sin\frac{\theta}{2} - 3\sin\frac{3\theta}{2}\right)\cdot K_{II}\right\} \tag{7}$$

$$\sigma_\theta = \frac{1}{\sqrt{2\pi r}}\left\{\frac{1}{4}\left(3\cos\frac{\theta}{2} + \cos\frac{3\theta}{2}\right)\cdot K_I - \frac{3}{4}\left(\sin\frac{\theta}{2} + \sin\frac{3\theta}{2}\right)\cdot K_{II}\right\} \tag{8}$$

$$\tau_{r\theta} = \frac{1}{\sqrt{2\pi r}}\left\{\frac{1}{4}\left(\sin\frac{\theta}{2} + \sin\frac{3\theta}{2}\right)\cdot K_I + \frac{1}{4}\left(\cos\frac{\theta}{2} + 3\cos\frac{3\theta}{2}\right)\cdot K_{II}\right\} = -\frac{2}{3}\frac{\partial\sigma_\theta}{\partial\theta} \tag{9}$$

where σ_r is the radial, σ_θ is the tangential, and $\tau_{r\theta}$ is the shear stress components. These expressions are valid both for plane stress and plane strain. The $\sigma_{\theta max}$ criterion assumes that crack growth begins on a plane perpendicular to the direction in which σ_θ is maximum. The maximum value of σ_θ is obtained when $\partial\sigma_\theta/\partial\theta$ is zero, or when (which is equivalent) $\tau_{r\theta} = 0$. This equation has a trivial solution $\theta = \pm\pi$ (for $\cos(\theta/2) = 0$), and a non-trivial solution $\theta = \theta_0''$ given by

$$\theta_0'' = 2\arctan\left(\frac{1}{4}\frac{K_I}{K_{II}} \pm \frac{1}{4}\sqrt{\left(\frac{K_I}{K_{II}}\right)^2 + 8}\right) \tag{10}$$

where the sign of θ_0'' is the opposite of the sign of $\mathbf{K}_{II}$. According to the $\sigma_{\theta max}$ criterion, the equivalent SIF is calculated at the value $\theta = \theta_0''$, which maximizes the expression

$$K_{eq} = \frac{1}{4}\left(3\cos\frac{\theta}{2} + \cos\frac{3\theta}{2}\right)\cdot K_I - \frac{3}{4}\left(\sin\frac{\theta}{2} + \sin\frac{3\theta}{2}\right)\cdot K_{II} \tag{11}$$

Several similar criteria have been proposed, e.g. by Nuismer, by Amestoy et al., by Richard, by Schöllmann et al., and by Pook, as comprehensively reviewed in [14]. A few of these criteria even predict the warping angle of a 3-D crack subject to Mode III loading. These models have notable differences if the amount of Mode II loading is significant. For instance, under pure Mode II loading, the propagation angle θ is $\pm 70.5^o$, $\pm 75^o$ and $\pm 82^o$ according to the $\sigma_{\theta max}$, $\mathbf{G}_{max}$ and $\mathbf{S}_{min}$ models, leading to $\mathbf{K}_{eq}$ values of approximately $\mathbf{1.15}\cdot\mathbf{K}_{II}$, $\mathbf{1.60}\cdot\mathbf{K}_{II}$ and $\mathbf{1.05}\cdot\mathbf{K}_{II}$ (assuming $\nu = \mathbf{0.3}$), respectively, while Tanaka predicts $\mathbf{K}_{eq} = \mathbf{1.68}\cdot\mathbf{K}_{II}$, and the **G**-based Equation (4) $\mathbf{K}_{eq} = \mathbf{K}_{II}$. The values of θ and $\mathbf{K}_{eq}$ obtained from each model are plotted in Figs. 1 and 2 as a function of the $\mathbf{K}_{II}/\mathbf{K}_I$ ratio.

The differences among the studied models might be significant for mixed-mode fracture predictions, however they turn out to be negligible for fatigue crack propagation calculations. In fact, since all above models predict crack path deviation ($\theta \neq 0$) under any $\mathbf{K}_{II}$ different than zero (see Fig. 2), they all imply that fatigue cracks will always attempt to propagate in pure Mode I, minimizing the amount of Mode II loading, curving their paths if necessary to avoid rubbing their faces. As soon as the crack path is curved to follow pure Mode I, all models agree that $\mathbf{K}_{eq}$ is equal to $\mathbf{K}_I$. Therefore, not only the crack path but also the associated SIF values calculated by any of the above criteria are essentially the same. This has been verified by Bittencourt et al. [7], who concluded from FE simulations that these criteria provide basically the same numerical results. Since the Maximum Circumferential Stress

criterion is the simplest, even presenting a closed form solution, it is the one adopted in the present work.

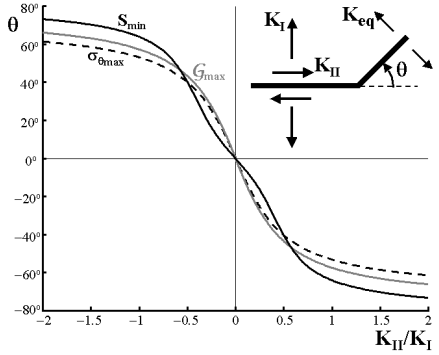

Figure 1: Crack propagation direction θ as a function of the $\mathbf{K}_{II}/\mathbf{K}_I$ ratio according to the $\sigma_{\theta max}$, $\mathbf{G}_{max}$ and $\mathbf{S}_{min}$ criterea.

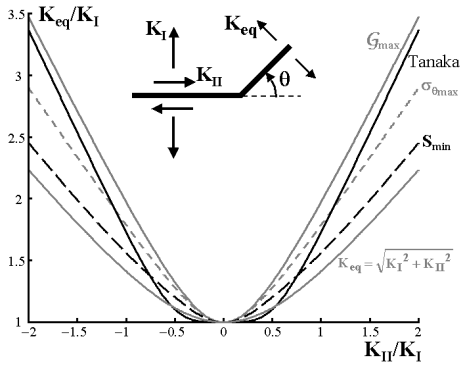

Figure 2: Equivalent SIF $\mathbf{K}_{eq}$ as a function of the $\mathbf{K}_{II}/\mathbf{K}_I$ ratio according to several models.

3 Numerical procedure

Two complementary pieces of software, named **Quebra** and ViDa [1, 15, 16], have been developed to implement the two steps of this hybrid methodology.

Quebra is an interactive graphical program for simulating two-dimensional fracture processes based on a FE self-adaptive mesh-generation strategy [15, 17]. This program includes all methods described above to compute the crack increment direction and the associated stress-intensity factors along the crack path. Moreover, its adaptive FE analyses are coupled with modern and very efficient automatic remeshing schemes, which substantially decrease the computational effort. The automatic calculation procedure in **Quebra** is performed in 4 steps: (i) the FE model of the cracked structure is solved to obtain $\mathbf{K}_I$ and $\mathbf{K}_{II}$ and to calculate the corresponding crack propagation direction; (ii) the crack is increased in the growth direction by a (small) required step; (iii) the model is remeshed to account for the new crack size; and (iv) the process is iterated until rupture or until a specified crack size is reached. As a result, a list of $\mathbf{K}_I$ and $\mathbf{K}_{II}$ values is generated at short but discrete intervals along the predicted crack paths.

The second program, named ViDa, is a general-purpose fatigue design program developed to predict both initiation and propagation fatigue lives under VA loading by all classical design methods, including the **SN**, the **IIW** (for welded structures) and the ε**N** for crack initiation, and the **da/dN** for crack propagation. It includes several load interaction models to predict overload and underload-induced crack retardation and acceleration. The program includes comprehensive database with mechanical properties of more than 13000 materials, hundreds of editable $\mathbf{K}_I$ and $\mathbf{K}_{II}$ SIF expressions and **da/dN** curves to be used in the calculations. In particular, ViDa accepts any crack growth equation and any SIF expression, making it an ideal companion to **Quebra**, which can be used to generate the required $\Delta\mathbf{K}$ expression if not available in its database.

4 Experimental results

The FCG experiments were performed on C(T) specimens of cold-rolled AISI 1020 steel with yield strength $\mathbf{S}_Y$ **= 285MPa**, ultimate strength $\mathbf{S}_U$ **= 491MPa**, Young modulus **E = 205GPa**, and reduction in area **RA = 54%**, measured according to the ASTM E 8M-99 standard, and with the analyzed weight percent composition: 0.19C, 0.46Mn, 0.14Si, 0.11Cu, 0.052Ni, 0.045Cr, 0.007Mo, 0.002Nb, 0.002Ti, Fe balance. The tests were performed at two **R = Kmin/K**$_{max}$ ratios, **R = 0.1** and **R = 0.7**, in a 250kN computer-controlled servo-hydraulic testing machine. The crack length was measured following ASTM E 647-99 procedures. The measured growth rates on 16 standard compact tension C(T) test specimens were fitted by a modified McEvily **da/dN** equation (in m/cycle), as shown in Figure 3, where the propagation threshold under **R = 0** is g$\Delta\mathbf{K}_0$ **= 11.5 MPa**$\sqrt{\mathbf{m}}$, and the fracture toughness is $\mathbf{K}_C$ **= 280 MPa**$\sqrt{\mathbf{m}}$.

Three modified C(T) specimens were designed and tested, with width **w = 29.5mm** and thickness **t = 8mm**. Each one had a 7mm-diameter hole positioned at a slightly different horizontal distance **A** and vertical distance **B** from the notch root, as shown in Figure 4(a). Two very different crack growth behaviors had been predicted by the FE modeling of the C(T) specimens, depending on the hole position. The predictions indicated that the fatigue crack was always attracted by the hole, but it could either curve its path and grow toward the hole ("sink in the hole" behavior) or just be deflected by the hole and continue to propagate after missing it ("miss the hole" behavior).

Using the **Quebra** program, the transition point between the "sink in the hole" and the "miss

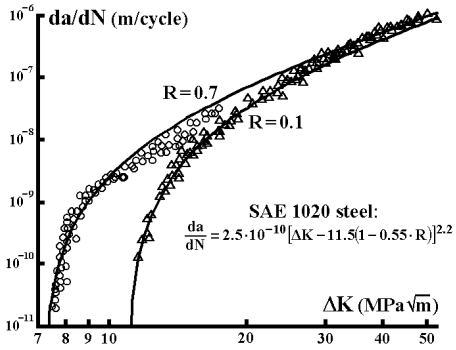

Figure 3: Modified McEvily **da/dN** equation fitted to the SAE 1020 steel data.

the hole" crack growth behaviors was identified. The three modified C(T) specimens were designed so that specimens named CT1(CA) and CT1(VA) had the hole just half a millimeter above the transition point, and a specimen named CT2(CA) had the hole half a millimeter below it. The chosen specimen geometries were machined, measured, and FE remodeled, to account for small deviations in the machining process (Figure 5). In this way, it could be assured that the numerical models used in the predictions reproduced the real geometry of the tested specimens.

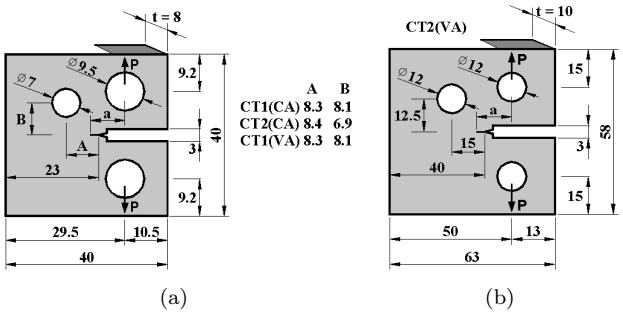

Figure 4: Measured dimensions of the hole-modified C(T) specimens (mm).

Specimens CT1(CA) and CT2(CA) were tested under CA loading, under a quasi-constant stress-intensity range $\Delta \mathbf{K}_I \approx \mathbf{20MPa}\sqrt{\mathbf{m}}$ and load ratio $\mathbf{R = 0.1}$.

Two specimens were tested under VA loading: one standard C(T) specimen, and the holed CT1(VA). The VA load histories applied to the specimens are shown in Figure 6.

Figure 7 shows the predicted and measured crack paths for the three modified specimens (in mm) under CA or VA loading, presenting a very good match. This suggests that the curved crack paths

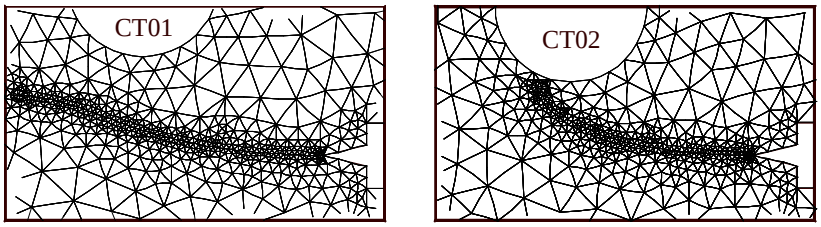

Figure 5: Automatically generated FE mesh of the CT1(CA) and CT2(CA) specimens.

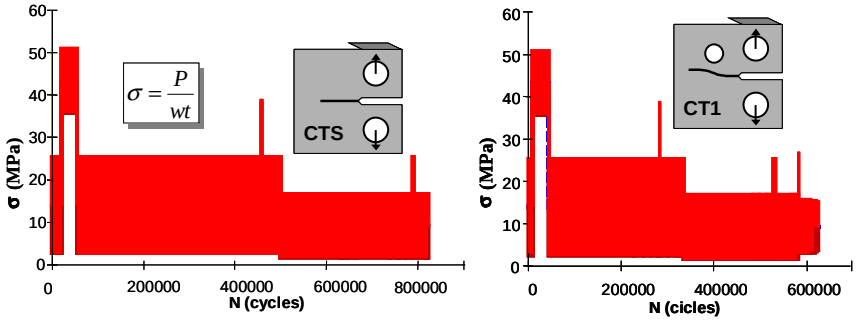

Figure 6: Applied load history (in kN) for standard C(T) and modified CT1(VA).

predicted under CA loading give good estimates of the measured paths under VA loading. Therefore, assuming that the Linear Elastic Fracture Mechanics (LEFM) conditions apply, the discussed two-step methodology can be generalized to the VA loading case.

The SIF values calculated under CA loading along the crack path using the **Quebra** program were exported to the ViDa software to predict fatigue life, considering load interaction effects.

Figure 8 shows predicted and measured crack sizes for the modified C(T) specimens under CA loading.

Several crack retardation models were calibrated based on the standard C(T) data under VA loading, including the Constant Closure model [11] (where the crack opening load $\mathbf{K}_{op}$ was calibrated as 26% of the maximum overload SIF, $\mathbf{K}_{ol,max}$), a modified Wheeler model [18, 19] (where the model's exponent was estimated as **0.51**), and Newman's closure model [20] (generalized for the VA loading case, where the stress-state constraint factor was fitted as αg **1.07**, suggesting dominant plane-stress FCG conditions). The fitted load interaction parameters were then used to predict in the ViDa program the crack growth behavior under VA loading of the hole-modified CT1(VA) specimen, see Fig. 9. The significant retardation effects of the CT1(VA) specimen were very well predicted using these three load interaction models.

Finally, a larger modified C(T) specimen named CT2(VA) has been designed and tested under VA

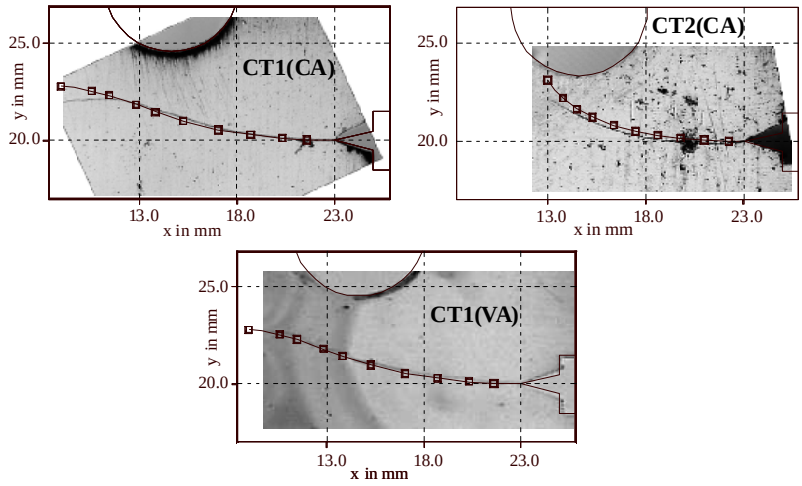

Figure 7: Predicted and measured crack paths for the modified C(T) specimens (mm).

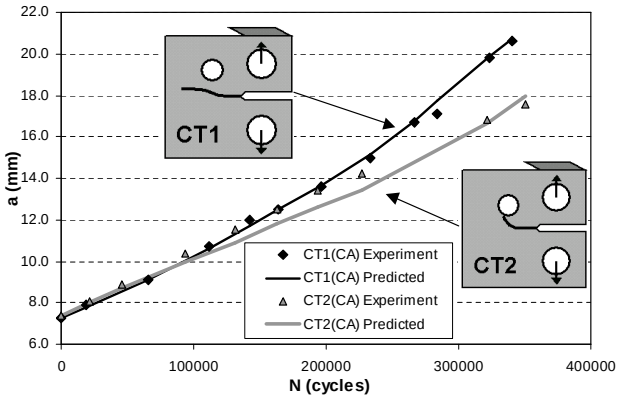

Figure 8: Predicted and measured FCG for modified C(T) specimens under CA loading.

loading, with sizes shown in Figure 2(b). The applid VA load history is shown in Fig. 10. As seen in Fig. 11(a), in the beginning there is a good match between the predicted and measured crack paths. However, after an overload at about 750,000 load cycles in the history, there is a significant deviation in the crack path. After carefully examining the specimen surface, it was found that the crack tip had unexpectedly bifurcated due to the overload, see Fig. 11(b). Even though such crack bifurcations can be easily modeled using the **Quebra** program [21, 22], it is very difficult to predict whether and when they are induced. In addition, this overload generated a very large plastic zone ahead of the

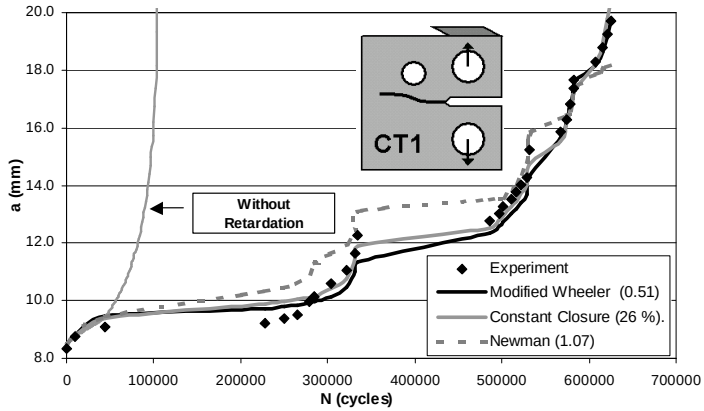

Figure 9: Crack growth predictions (based on straight-crack calibrations) on a modified C(T) specimen under VA loading.

bifurcated crack tip, with dimensions comparable to the length of the residual ligament between the crack and the hole, invalidating LEFM assumptions. Thus, elastic-plastic FE calculations considering bifurcation effects would be required to predict the crack path of this specimen.

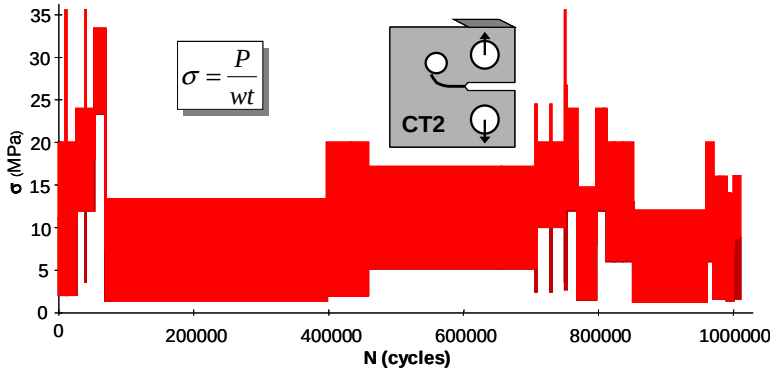

Figure 10: Applied load history for standard modified CT2(VA) specimens.

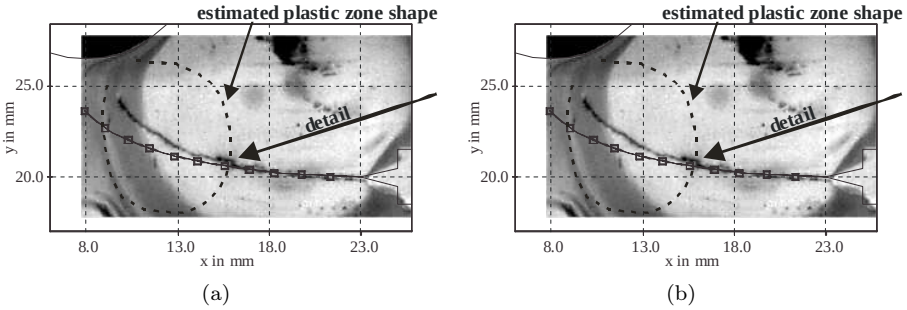

Figure 11: Predicted and measured crack paths for the CT2(VA) specimens.

5 Conclusion

A two-phase methodology was presented to predict fatigue crack propagation in generic 2D structures. First, self-adaptive finite elements were used to calculate the fatigue crack path and the stress-intensity factors along the crack length $\mathbf{K}_I\mathbf{(a)}$ and $\mathbf{K}_{II}\mathbf{(a)}$, at each propagation step. The computed $\mathbf{K}_I\mathbf{(a)}$ was then used to calculate the propagation fatigue life by the local approach, considering overload-induced crack retardation effects.

Two complementary software have been developed to implement this methodology. The first is an interactive graphical program for simulating two-dimensional fracture processes based on a finite-element adaptive mesh-generation strategy. The second is a general-purpose fatigue design software developed to predict both initiation and propagation fatigue lives under variable loading by all classical design methods. Particularly, its crack propagation module accepts any stress-intensity factor expression, including the ones generated by the finite-element software.

Experimental results validated the proposed methodology, in particular suggesting that overloads do not significantly deviate the crack path predicted under simple loading. Moreover, the developed software demonstrated that effective and economical predictions of crack propagation paths and fatigue lives can be obtained for arbitrary two-dimensional structural components under variable amplitude loading, provided that they did not induce crack bifurcation or plastic zones with sizes comparable to the residual ligament.

References

[1] Miranda, A.C.O., Meggiolaro, M.A., Castro, J.T.P., Martha, L.F. & Bittencourt, T.N., Fatigue crack propagation under complex loading in arbitrary 2d geometries. *ASTM STP*, **1411(4)**, pp. 120–145, 2002.

[2] Shih, C.F., de Lorenzi, H.G. & German, M.D., Crack extension modeling with singular quadratic isoparametric elements. *Int Journal of Fracture*, **12**, pp. 647–651, 1976.

[3] Raju, I.S., Calculation of strain-energy release rates with higher order and singular finite elements. *Engineering Fracture Mechanics*, **28**, pp. 251–274, 1987.

[4] Rybicki, E.F. & Kanninen, M.F., A finite element calculation of stress-intensity factors by a modified crack closure integral. *Eng Fracture Mechanics*, **9(931-938)**, 1977.
[5] Dodds Jr., R.H. & Vargas, P.M., Numerical evaluation of domain and contour integrals for nonlinear fracture mechanics. Technical report, Dept. of Civil Engineering - Univ. of Illinois, Urbana-Champaign, 1988.
[6] Nikishkov, G.P. & Atluri, S.N., Calculation of fracture mechanics parameters for an arbitrary three-dimensional crack by the equivalent domain integral method. *International Journal for Numerical Methods in Engineering*, **24**, pp. 1801–1821, 1987.
[7] Bittencourt, T.N., Wawrzynek, P.A., Ingraffea, A.R. & Sousa, J.L.A., Quasi-automatic simulation of crack propagation for 2d lefm problems. *Eng Fracture Mechanics*, **55**, pp. 321–334, 1996.
[8] McEvily, A.J., Current aspects of fatigue. *Metal Science*, **11**, pp. 274–284, 1977.
[9] Tanaka, K., Fatigue propagation from a crack inclined to the cyclic tensile axis. *Eng Fracture Mechanics*, **6**, pp. 493–507, 1974.
[10] Irwin, G.R., Analysis of stresses and strains near the end of a crack transversing a plate. *J Applied Mechanics*, **24**, pp. 361–370, 1957.
[11] Hussain, M.A., Pu, S.U. & Underwood, J., Strain energy release rate for a crack under combined mode i and ii. *ASTM STP*, **560**, pp. 2–28, 1974.
[12] Sih, G.C., Strain-energy-density factor applied to mixed mode crack problems. *Int Journal of Fracture Mechanics*, **10(305-321)**, 1974.
[13] Erdogan, F. & Sih, G.C., On the crack extension in plates under plane loading and transverse shear. *Journal of Basic Engineering*, **85**, pp. 519–527, 1963.
[14] Richard, H.A., Theoretical crack path determination. *Int. Conference on Fatigue Crack Paths*, Parma - Italy, 2003.
[15] Miranda, A.C.O., Meggiolaro, M.A., Castro, J.T.P., Martha, L.F. & Bittencourt, T.N., Fatigue life and crack path prediction in generic 2d structural components. *Engineering Fracture Mechanics*, **70**, pp. 1259–1279, 2003.
[16] Meggiolaro, M.A. & Castro, J.T.P., Vida - a visual damagemeter to automate the fatigue design under complex loading. *Journal of the Brazilian Society of Mechanical Sciences*, **20**, pp. 666–685, 1998.
[17] Wawrzynek, P.A. & Ingraffea, A.R., Interactive finite element analysis of fracture processes: An integrated approach. *Theor Appl Fract Mech*, **8**, pp. 137–150, 1987.
[18] Wheeler, O.E., Spectrum loading and crack growth. *J Basic Eng*, pp. 181–186, 1972.
[19] Meggiolaro, M.A. & Castro, J.T.P., An evaluation of elber-type crack retardation models. *SAE*, **(SAE #2001-01-4063)**, pp. 207–216, 2001.
[20] Newman Jr., J.C., A crack opening stress equation for fatigue crack growth. *Int Journal of Fracture*, **24(3)**, pp. R131–R135, 1984.
[21] Meggiolaro, M.A., Miranda, A.C.O., Castro, J.T.P. & Martha, L.F., Stress intensity factor equations for branched crack growth. *Engineering Fracture Mechanics*, **72(17)**, pp. 2647–2671, 2005.
[22] Meggiolaro, M.A., Miranda, A.C.O., Castro, J.T.P. & Martha, L.F., Crack retardation equations for the propagation of branched fatigue cracks. *International Journal of Fatigue*, **27(10-12)**, pp. 1398–1407, 2005.